Chapter 7. Fibril alignment in liquid crystalline mesophases and extracellular matrices.

In general, biological molecules self-assemble via polar electrostatic interactions in an aqueous environment. Filamentous molecules may be covered by a sheath of polar water molecules and aligned by fluid shear. For example, silk fibroin is stored as a liquid crystalline mesophase, before the stress-alignment of filaments during their extrusion [1]. Similarly, praying mantid oothecal proteins are stored in liquid crystalline form before being secreted as a tanned foam around the egg cluster [2]. The oothecal protein fibrils are aligned in parallel, with a slight additional chiral torque, as a helicoidal liquid crystalline mesophase (Fig. 9). Helicoidal rotation is retained within droplets of oothecal fluid suspended in aqueous phosphate buffer. However, the pitch of the helicoidal laminae is constrained by the topography of the droplet/buffer interface, with long-range fibril alignment, and liquid crystalline disclinations (Figs. 9, 10). In general, the chiral (helicoidal) torque may result from dipole-dipole interactions between optically active molecules, with induced (dipole-quadrupole) interactions through a superficial layer of polar water molecules [4].

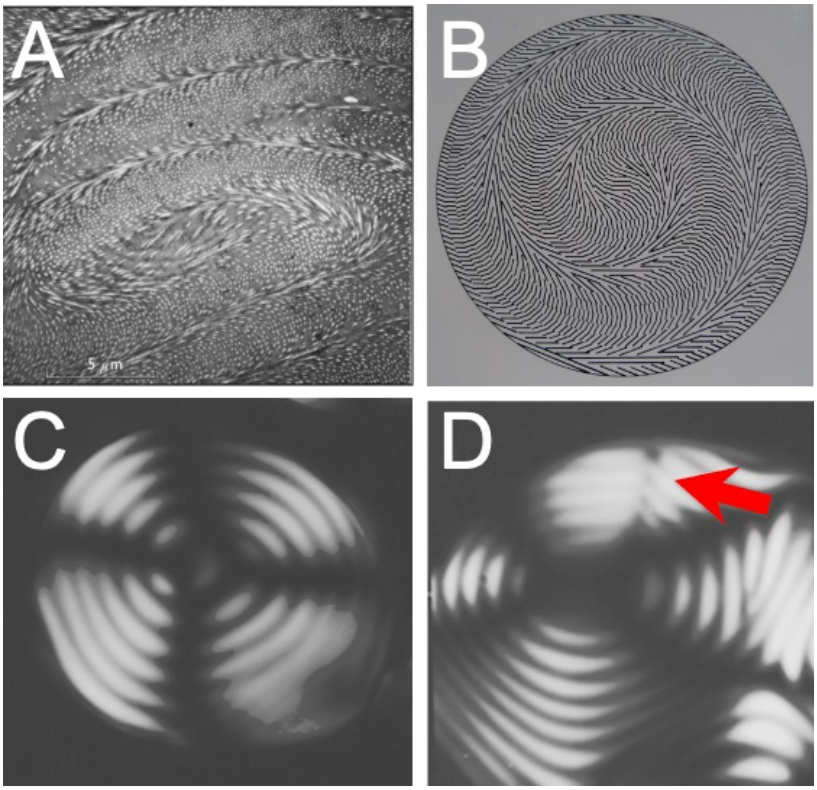

Fig. 9. Double-spiral pattern in helicoidal spheres. A. Section through spherical helicoidal domain in fixed mantid oothecal protein showing electron-light fibrils, TEM, magnification 6500X, from Neville and Luke, 1971. **B.** Diagram of double-spiral alignment of fibrils through the equatorial plane of an helicoidal sphere. **C.** Spherical droplet of oothecal protein suspended in phosphate buffer, viewed between crossed polaroid filters. The optically anisotropic fibrils block transmission of plane polarised light, such that rotated protein filaments show a double-spiral configuration. **D.** Spherical helicoidal droplet of oothecal protein between crossed polaroid filters showing unique radial stacking flaw (red arrow) D. Gubb, unpublished, as predicted by Pryce and Frank, 1957.

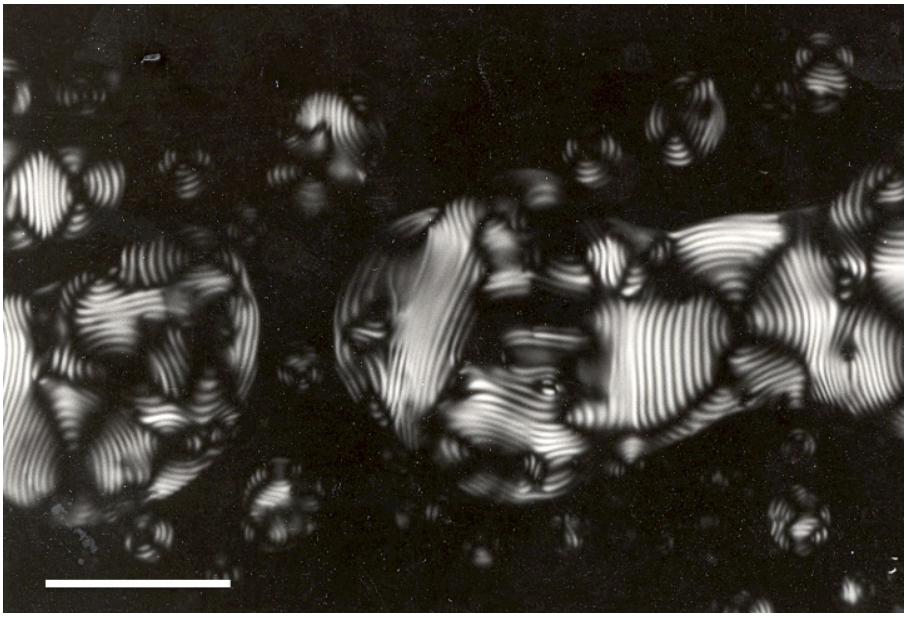

Fig. 10. Mantis oothecal protein droplets. The liquid crystalline filaments are in alignment across extended domains, white bar = 100 μ. The pitch of the helicoidal laminae, and topological disclinations, may be constrained by surface boundary effects at the oothecal protein/buffer interface. Protein droplets suspended in phosphate buffer, between siliconised glass slide and coverslip; Axiophot light microscope with crossed polaroid filters. D. Gubb, unpublished.

Rotated, helicoidal laminae of chitin fibrils form the major fibrillar component of arthropod cuticle [3 4 5] (Fig. 11).

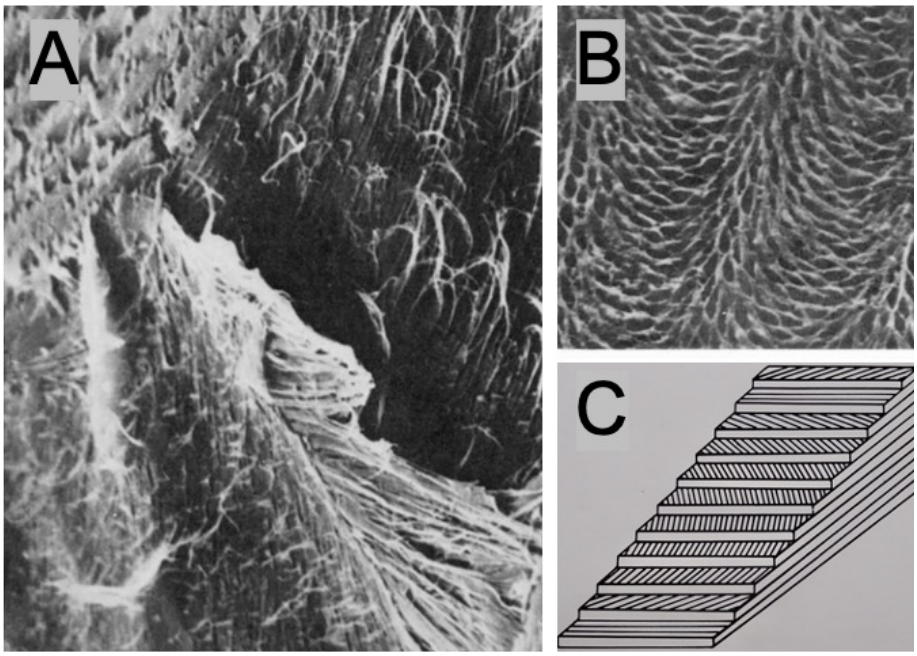

Fig. 11. Helicoidal chitin laminae in crab cuticle. SEM of microtome cut sections of decalcified and deproteinated cuticle. **A.** Section in laminar plane. **B.** Section tangential to laminar plane, the pore canals trace arced trajectories through the shrunken, chitinous matrix. **C.** Wedge diagram of rotated helicoidal laminae in tangential section. From Gubb, 1975.

Notably, the helicoidal chitin laminae in some metallic-coloured beetles reflects, left-circularly polarised light, with a wavelength dependent on the pitch of the rotated fibrils, Fig.12.

Fig. 12. Optically active Scarabeid beetle exocuticle. Left circularly polarised light is reflected as it passes through helicoidal chitin lamellae, with wavelengths dependent on the helicoidal pitch. The coloured patterns are bilaterally symmetrical, although lamellar rotation is right-handed on both sides of the body. From, Neville and Caveney, 1969.

The first layer of extracellular chitin fibrils is symmetrical around the L/R mid-line of the beetle, but this bilateral symmetry is lost in subsequent rotated layers [6 7]. By implication, both the laminar pitch and the shape of the exoskeleton are dependent on self-assembling components secreted from the underlying epithelium. Arthropod cuticle is acellular, but vertical pore canals traverse its thickness in an hexagonal array of flat, twisted ribbons; with corkscrew trajectories through the rotated helicoidal laminae [6 5], (Fig. 11). The pore canals may contain filopodial extensions [4], which would allow the export of extracellular matrix components from the underlying epithelium. Notably, the rotated helicoidal laminae show no discontinuities above the lateral cytoplasmic interfaces of the epithelial cells.

By contrast to the arthropods, the extracellular matrix fibrils of many multicellular organisms are collagenous. The collagen fibrils in mammalian skin tend to be aligned with the epithelial surface, but with random orientation in the surface plane. However, collagen fibrils are aligned preferentially along lines of stress in tendons and bone; they form 2D orthogonal plies in fish scales and in 2D, or 3D, orthogonal lattices in annelid cuticle [8 9 10]. Collagen fibrils may reassemble from aqueous solution *in vitro*, with charged, electropositive bands in register; and with parallel, or orthogonal, alignment [10]. In the vertebrate cornea, collagen fibrils form rotated laminae within in a deformable fluid matrix of the same refractive index. An initial layer of one, or a few, parallel collagen fibrils is aligned against the surface of the primary corneal epithelium [11 12]. Subsequent layers remain one, or a few, collagen fibrils thick; with each layer aligned orthogonally to the previous layer, but with a slight incremental rotation, Fig. 13 [12 13]. As in insect cuticle, the fibril orientation of the initial layer is symmetrical around the body mid-line, with an anticlockwise helicoidal rotation in both L and R corneas.

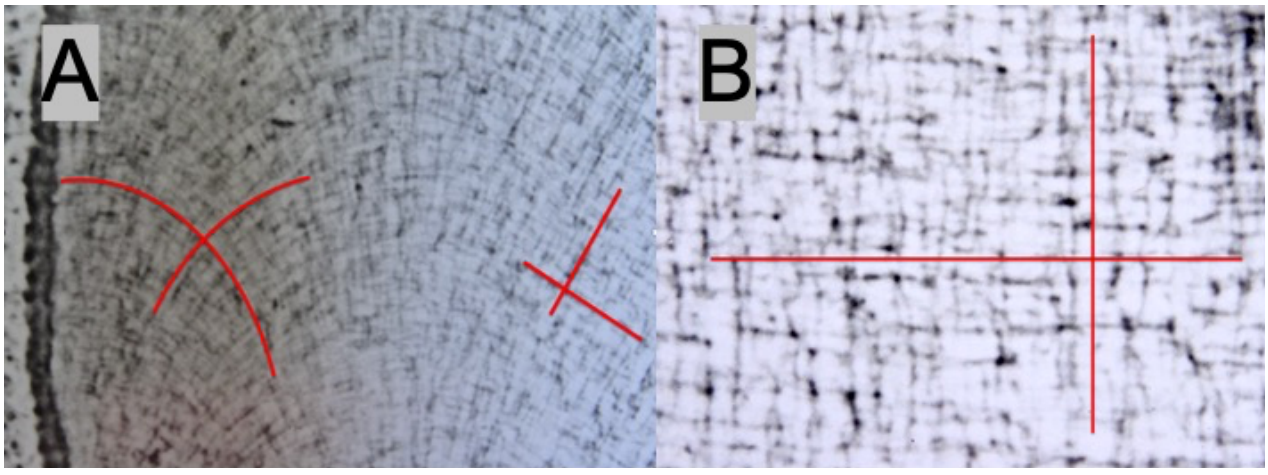

Fig. 13. Rotated collagen laminae in chick cornea. Collagen fibrils of primary corneal stroma, wax microtome sections stained with Gomori silver stain **A.** Successive collagen filaments are close to orthogonal, but slightly off-set from 90º. Towards the perimeter of the cornea, the knife section is tangential to the fibril layers, showing curved arcs of rotated orthogonal collagen fibrils, curved red lines. Near the centre of the section, the knife section is in the plane of the collagen fibrils, showing an orthogonal mesh, crossed red lines. However, the collagen fibrils may remain slightly off-set from 90º. **B.** Enlargement of central region of section. The occasional black dots at collagen lattice intersections, may correspond to keratocytes. D. Gubb and J. Dodson, unpublished.

After formation of the primary stroma, keratocytes migrate within the matrix and secrete further pro-collagen fibrils, which assemble in parallel to the template layers [14]. This two-step mechanism allows the rapid growth of mechanically and optically isotropic tissue. Additional collagen filaments pass vertically through the rotated layers [12] like the arthropod pore canals. The anticlockwise helicoidal rotation of the chick corneal lens can be reversed, in both eyes, during secretion of the primary stromal layers by the chiral glutamine analogue DON [15]. The simplest hypothesis may be that the first layer of fibrils is aligned by epithelial surface contours and non-Newtonian fluid shear. Subsequent, short bursts of pro-collagen secretion may assemble fibrils with an orthogonal alignment to the previous template layer, with a slight addition twist generated via polar, aqueous interactions. Thus, nascent fibrils may align in parallel with each other; against the striated, charged bands of the mature, cross-linked collagen filaments [16].

The first stage of pro-collagen assembly takes place within the Golgi and rough ER [17]. In these intracellular compartments, the collagen pro-peptides form entwined, triple-helical coils, with each chain staggered by one residue with respect to the next [18 19]. The assembly of the triple-helical collagen fold is driven by electrostatic interactions between proline and glycine residues, which lack peptide side chains. Most pro-collagens carry additional disordered segments, with N and C-terminal extensions that are proteolytically cleaved before fibril maturation. However, truncated human $\alpha 1$ and $\alpha 2$ collagens can assemble when co-expressed (and secreted from) yeast cells, although their fibril diameter is irregular, with only short lengths of polar residues in register [20]. A synthetic $(Pro\text{-}Pro\text{-}Gly)_{10}$ oligomer assembles as a triple left-handed helix, with polar bonds between Gly and Pro residues in adjacent chains. In this 3X entwined fold, the carbonyl groups of the polymer chains are solvent-exposed and hydrated; while their N and C termini carry positive and negative charges, respectively. In consequence, the triple-helical, micro-filaments assemble with alternating head-to-tail orientations [21]. In native collagen fibrils, the triplet repeats consist of X-Y-Gly, with the X and Y residues being predominantly Pro. Every third residue is Gly, while one of the two Pro residues may be hydroxylated, Pr^{OH}. Fibrils tend to be stabilised by Pr^{OH} in the Y position and destabilised by Pr^{OH} in the X position [22]. Thus, post-translational modification may be critical during fibril assembly, although short lengths of disordered fibril may re-assemble *in vitro* in the absence of prolyl hydroxylase [20 23]. In general, native triple-helical microfilaments consist of 20X stretches of the X-Y-Gly repeat, interspersed with disorganised domains to which glycosylated side chains may be attached. The 20x triplet repeats stack in register, to form a braided rope of cylindrical fibrils with orthogonal rings of charged residues around their diameter. However, the triple helical braids assemble with interspersed disorganised domains such that the succession of $(X\text{-}Y\text{-}Gly)_{20}$ domains may not be co-linear with the primary peptide sequence [24].

In this context, the braided microfilaments of bovine corneal collagen form extended, cylindrical rods packed within a right-handed supercoiled cylinder, with a pitch of about 15º and an axial repeat of 67 nm. The surface-bound components include Leucine Rich Repeat (LRR) proteo-glycans, which may bind to N- and C-terminal collagen peptides [25]. The periodic attachment of bulky LLR sidechains to the mature collagen fibril may block the subsequent parallel alignment of nascent fibrils, while leaving exposed charged bands around the braided triple-helical repeats. Thus, orthogonal fibrils may be nucleated, and aligned, between the LLR sidechains of mature, cross-linked, collagen fibrils. Notably, denatured collagen tends to re-assemble as parallel filaments in the absence proteoglycans [26]. An additional chiral, helical twist may be generated between the polar H_2O sheath of the triple-helical collagen domains and other matrix components, as in cholesteric mesophases. In this context, during cooling of cholesteryl benzoate, liquid crystalline phase transitions take place from parallel (nematic) alignment to rotated (helicoidal) to “blue phase”, Reiner 1888, see [27]. This blue phase consists of helicoidally-wound tubular rods of indefinite length, with orthogonal intersections within a 3D lattice [28]. Similar 3D lattice intersections might link braided collagen microfibrils

at a much larger scale, with swapping of triple helical domains between microfibrils at lattice intersections. Such a mechanism would allow the assembly of an orthogonal fibrillar mesh, with interchanged 3X collagen domains without lattice disclinations. Strikingly, the collagen fibrils in annelid cuticle can form helicoidal laminae, or a 3D "blue phase" lattice of braided helicoidal fibrils [8] [10]. Similarly, the radial collagen fibrils that transverse the depth of vertebrate corneal lens may trace a twisted, corkscrew pitch through the rotated helicoidal layers, as in arthropod cuticle. Such blue phase architecture might facilitate the uniform distribution of keratocytes through the secondary corneal stroma, see Fig.11C, 12 [12]. In this respect, the migrating keratocytes are essentially apolar, with the matrix components that they secrete being aligned against the primary template layers.

The alignment of an initial layer of collagen filaments may template extracellular matrix assembly, and other filamentous molecules. Thus, collagen fibrils may regulate the fine-scale topography of epithelial surfaces and constrain the assembly of extra-cellular matrix components. Uniform, parallel undulae run across the epithelial supported by straight microtubule bundles during embryonic cuticle secretion in Drosophila [29]. The chiral twist between the chitin fibrils in arthropod cuticle may be driven by polar aqueous interactions. However, the pitch of the helicoidal laminae is controlled from the underlying epithelium, together with secreted glycosaminoglycans and additional protein components. In this context, the cognate *viking* (*vkg*) and *Col4a* genes mediate exocytosis, via Dpp (Decapentaplegic, aka: TGFα, Bone Morphogenetic Protein) [30] [31] [32]. In particular, the phenotypes associated with *Col4a* mutants in *Drosophila* resemble human collagen-disease syndromes, including a LOF collagen myopathy [33] [34]. By these criteria, collagen-dependent morphogenetic functions are strongly conserved during the secretion and self-assembly of extracellular matrices.

Summary:

The fibrils of extracellular matrices tend to be aligned with the surface plane of underlying epithelial layers. Fibrils of the initial layer may be aligned against the epithelial surface contours, without discontinuities at lateral cell boundaries, but with mirror symmetric orientations around the L/R midline. Subsequent layers assemble against the initial template, with fibril alignment via polar electrostatic interactions and non-Newtonian fluid shear. Collagen fibrils can re-assemble in either parallel or orthogonal arrays *in vitro* and may have a critical template function for other matrix components *in vivo*. In arthropod cuticle and vertebrate corneas, a slight chiral rotation may drive the assembly of rotated laminae, with the loss of bilaterally symmetrical fibril orientations in subsequent layers. The initial assembly of pro-collagen takes place within the Golgi apparatus. Alignment of the collagen triple-helical fold is driven by electrostatic charge asymmetry, transmitted through a polar sheath of water molecules. The pro-collagen sub-units assemble into braided collagen filaments, with charged cylindrical bands, against which additional parallel, or orthogonal, filaments, may align. In arthropods, collagen scaffolds may template the assembly of chitin fibrils, with an additional chiral rotation in the epithelial plane. Vertical pore canals penetrate the rotated laminae, with filopodial extensions through which matrix components may be exported. An analogous mechanism may form the rotated, orthogonal plies in the vertebrate cornea; with motile, apolar cells able to migrate along the collagen scaffold. These more complex fibrillar architectures may be dependent on hexagonal tessellation of the underlying epithelial layer, with 3D scaffolds resembling blue-phase cholesteric mesophases. Thus, the collagen triple-helical fold may drive assembly of uniform, parallel filaments, or orthogonal arrays, at epithelial/matrix interfaces.

References:

1. Vollrath, F. & Knight, D. P. Liquid crystalline spinning of spider silk. *Nature* **410**, 541 548 (2001).
2. Neville, A.C. & Luke, B.M. A biological system producing a self-assembling cholesteric protein liquid crystal. *J. Cell Sci. 81 Pp93-109* **8**, 93–109 (1971).
3. Bouligand, Y. Twisted fibrous arrangements in biological materials and cholesteric mesophases. *Tissue Cell* **4**, 189–217 (1972).
4. Barth, F. G. Microfiber reinforcement of an arthropod cuticle. *Z. Für Zellforsch. Mikrosk. Anat.* **144**, 409–433 (1973).

5. Gubb, D. A direct visualisation of helicoidal architecture in Carcinus maenas and Halocynthia papillosa by scanning electron microscopy. *Tissue Cell* **7**, 19–32 (1975).
6. Neville, A. C., Thomas, M. G. & Zelazny, B. Pore canal shape related to molecular architecture of arthropod cuticle. *Tissue Cell* **1**, 183–200 (1969).
7. Neville, A. C. Cuticle ultrastructure in relation to the whole insect. *Symp. R. Entomol. Soc. Lond.* 17–39 (1970).
8. Lepescheux, L. Spatial organization of collagen in annelid cuticle: order and defects. *Biol. Cell* **62**, 17–31 (1988).
9. Traub, W., Arad, T. & Weiner, S. Three-dimensional ordered distribution of crystals in turkey tendon collagen fibers. *Proc. Natl. Acad. Sci.* **86**, 9822 (1989).
10. Gaill, F, F. Geometry of biological interfaces: the Collagen networks. *J Phys Colloq.* **51**, C7-169 (1990).
11. Trelstad, R. L. & Coulombre, A. J. Morphogenesis of the collagenous stroma in the chick cornea. *J. Cell Biol.* **50**, 840–858 (1971).
12. Young, R. D. *et al.* Cell-independent matrix configuration in early corneal development. *Exp. Eye Res.* **187**, 107772 (2019).
13. Gordon, H. Corneal geometry: An alternative explanation of the effect of 6-diazo-5-oxo-l-norleucine on the development of chick cornea. *Dev. Biol.* **53**, 303–305 (1976).
14. Young, R. D. *et al.* Three-dimensional aspects of matrix assembly by cells in the developing cornea. *Proc. Natl. Acad. Sci.* **111**, 687 (2014).
15. Coulombre, J & Coulombre, A.J. Corneal development V. Treatment of five-day old embryos of domestic fowl with 6-diazo-5-oxo-l-norleucine. *Devl Biol* **45**, 291–303 (1975).
16. Van Der Rest, M. & Garrone, R. Collagen family of proteins. *FASEB J.* **5**, 2814–2823 (1991).
17. Lerner, D. W. *et al.* A Rab10-dependent mechanism for polarized basement membrane secretion during organ morphogenesis. *Dev. Cell* **24**, 159–168 (2013).
18. Berisio, R., Vitagliano, L., Mazzarella, L. & Zagari, A. Crystal structure of the collagen triple helix model [(Pro-Pro-Gly)(10)](3). *Protein Sci. Publ. Protein Soc.* **11**, 262–270 (2002).
19. Hulmes, D. J. S. Building Collagen Molecules, Fibrils, and Suprafibrillar Structures. *J. Struct. Biol.* **137**, 2–10 (2002).
20. Olsen, D.R *et al. J. Biol. Chem.* **276**, 24038–24043 (2001).
21. Berisio, R, Vitagliano, L, Mazzarella, L, & Zagari, A. Crystal structure of the collagen triple helix model[(Pro-Pro-Gly)10]3. *Protein Sci.* **11**, 262–270 (2002).
22. Taga, Y., Tanaka, K., Hattori, S. & Mizuno, K. In-depth correlation analysis demonstrates that 4-hydroxyproline at the Yaa position of Gly-Xaa-Yaa repeats dominantly stabilizes collagen triple helix. *Matrix Biol. Plus* **10**, 100067 (2021).
23. Vitagliano, L., Berisio, R., Mazzarella, L. & Zagari, A. Structural bases of collagen stabilization induced by proline hydroxylation. *Biopolymers* **58**, 459–464 (2001).
24. Than, M. E. *et al.* The 1.9-Å crystal structure of the noncollagenous (NC1) domain of human placenta collagen IV shows stabilization via a novel type of covalent Met-Lys cross-link. *Proc. Natl. Acad. Sci.* **99**, 6607 (2002).
25. Holmes, D. F. *et al.* Corneal collagen fibril structure in three dimensions: Structural insights into fibril assembly, mechanical properties, and tissue organization. *Proc. Natl. Acad. Sci. U. S. A.* **98**, 7307–7312 (2001).
26. Graham, H. K., Holmes, D. F., Watson, R. B. & Kadler, K. E. Identification of collagen fibril fusion during vertebrate tendon morphogenesis. The process relies on unipolar fibrils and is regulated by collagen-proteoglycan interaction1 1Edited by M. F. Moody. *J. Mol. Biol.* **295**, 891–902 (2000).
27. Sluckin, T. J, Dunmur, David A, & Stegemeyer, Horst. *Crystals That Flow: Classic Papers from the History of Liquid Crystals*. (Taylor & Francis, London, 2004).
28. Coles, H. J. & Pivnenko, M. N. Liquid crystal 'blue phases' with a wide temperature range. *Nature* **436**, 997–1000 (2005).
29. Moussian, B., Seifarth, C., Müller, U., Berger, J. & Schwarz, H. Cuticle differentiation during Drosophila embryogenesis. *Arthropod Struct. Dev.* **35**, 137–152 (2006).
30. Blumberg, B., MacKrell, A. J. & Fessler, J. H. Drosophila basement membrane procollagen alpha 1(IV). II. Complete cDNA sequence, genomic structure, and general implications for supramolecular assemblies. *J. Biol. Chem.* **263**, 18328–18337 (1988).

31. Wang, X., Harris, R. E., Bayston, L. J. & Ashe, H. L. Type IV collagens regulate BMP signalling in Drosophila. *Nature* **455**, 72 (2008).
32. Sawala, A., Sutcliffe, C. & Ashe, H. L. Multistep molecular mechanism for Bone morphogenetic protein extracellular transport in the Drosophila embryo. *Proc. Natl. Acad. Sci. U. S. A.* **109**, 11222–11227 (2012).
33. Bunt, S. *et al.* Hemocyte-secreted type IV collagen enhances BMP signaling to guide renal tubule morphogenesis in Drosophila. *Dev. Cell* **19**, 296–306 (2010).
34. Kelemen-Valkony, I. *et al.* Drosophila basement membrane collagen col4a1 mutations cause severe myopathy. *Matrix Biol.* **31**, 29–37 (2012).